

## Kinetics of the $[\text{Fe}(\text{CN})_6]^{3-}/[\text{Fe}(\text{CN})_6]^{4-}$ Redox Couple Reaction on Anodically Passivated $\text{Fe}_{80}\text{B}_{20}$

*Višnja Horvat-Radošević, Krešimir Kvastek, and Dejana Križekar*

*Department of Physical Chemistry and Centre for Marine Research,  
Ruđer Bošković Institute, P.O. Box 1016, 10001 Zagreb, Croatia*

Received July 18, 1996; revised September 18, 1996; accepted September 19, 1996

The redox reaction of various concentrations (in 1 : 1 molar ratio) of the  $[\text{Fe}(\text{CN})_6]^{3-}/[\text{Fe}(\text{CN})_6]^{4-}$  redox couple in the neutral borate-buffered (pH = 8.4) electrolyte solution is studied on the  $\text{Fe}_{80}\text{B}_{20}$  electrode passivated under strongly defined conditions. Impedance measurements in the potentiostatic mode and »quasi« steady-state polarization measurements are used. The results of measurements clearly show the electron transfer reaction occurring as the rate determining reaction in both directions (cathodic and anodic) *vs.*  $R_{\text{rev}}$  of the redox couple. The rates of reactions as well as the value of the exchange current are low, but characteristic of the oxide-covered electrodes. The impedance data analysis reveals the electron transfer reaction impedance to be in parallel with an already existing passive film/solution interface impedance in the blank solution. Redox reaction on the passivated  $\text{Fe}_{80}\text{B}_{20}$  proceeds *via* electron transfer between the conduction band and ions in the solution, which is characteristic of the classical semiconductor of n-type. Contribution of either tunnelling of electrons across an electron depletion space-charge layer and/or electron transfer occurring partly *via* surface states is characteristic of the cathodic side of potentials. At anodic potentials, however, in the conditions of a thick space-charge layer acting as a high surface barrier, an electron transfer proceeds mainly *via* surface states being insured by ionization of donors within the passive film. In both ranges of potentials, the rate of reaction is determined predominantly by the solid side properties, and not by the properties of the ionic double layer present at the solution side of the passive film/solution interface. Comparison with literature data on (thick) anodic passive films formed on the pure iron points to similar kinetic data of two passive films, but to lower catalytic efficiency of the  $\text{Fe}_{80}\text{B}_{20}$  passive film surface.

## INTRODUCTION

In a series of previous papers, the electrochemical behaviour of anodically passivated glassy alloy  $\text{Fe}_{80}\text{B}_{20}$  electrode was thoroughly characterized by impedance measurements in acid sulphate,<sup>1,2</sup> near neutral borate,<sup>2,3</sup> and borate solutions of various pH of the electrolyte solution.<sup>4</sup> The best corrosion protective, slowly dissolving »true-passive« film of n-semiconductor type is formed on  $\text{Fe}_{80}\text{B}_{20}$  in near neutral borate-buffer solution. However, the films formed in acid sulphate solutions have much higher corrosion rates. Their »quasi-passive« characteristics are ascribed to the outer precipitated sulphate layer, which acts as the protective layer formed above the strongly dissolving oxide inner layer. Comparison with impedance data obtained on the pure passivated Fe has shown a detrimental effect of B on either corrosion properties or on the parameters of the oxygen evolution reaction (OER).

In the work described below, the electrochemical kinetics of the ferri-ferrocyanide redox reaction on the passivated  $\text{Fe}_{80}\text{B}_{20}$  is examined as a function of the potential and concentration of redox species in the borate-buffered (pH = 8.4) solution. The mechanism of the electron transfer reaction (ETR) is considered relevant in connection with the electronic properties of passive films which, if thick enough, may act as either ordinary semiconductors or insulators.<sup>5-8</sup>

The aim of this work is to establish the electron transfer mechanism of the redox couple on the passivated  $\text{Fe}_{80}\text{B}_{20}$  electrode, and to separate the parameters of the ETR, in order to determine the overall behaviour of the passivated  $\text{Fe}_{80}\text{B}_{20}$ . Its another aim is to confirm the sensitivity of the impedance method as a technique for the characterization of electrode surfaces.<sup>9</sup> The choice of the  $[\text{Fe}(\text{CN})_6]^{3-}/[\text{Fe}(\text{CN})_6]^{4-}$  redox couple is based on the well known arguments commonly emphasized in the relevant literature.<sup>5,10</sup> Thus,  $\text{K}_3\text{Fe}(\text{CN})_6$  and  $\text{K}_4\text{Fe}(\text{CN})_6$ , when present in the electrolyte solution, do not adsorb on an electrode surface, do not hydrolyze appreciably, and they have only two valence states available, so the reaction is the one-electron reaction. In addition, they are stable, their reversible potential falls in about the middle of the passive region of the  $\text{Fe}_{80}\text{B}_{20}$  electrode in the neutral solution, and their electrochemical parameters are relatively well established for the passivated iron electrode.<sup>6,7,10-16</sup>

## EXPERIMENTAL

### *Electrolytic Cell*

A conventional three-electrode electrolytic cell was used, with the working electrode being  $\text{Fe}_{80}\text{B}_{20}$ . The counter electrode was a Pt-spiral of high surface area, and the reference electrode was the saturated calomel electrode (SCE) with a Luggin capillary situated at about 1 mm from the centre of the working electrode. The cell was

thermostated at  $293 \pm 0.5$  K, the electrolyte solutions were always kept away from the light and continuously degassed with purified  $N_2$  prior to and during measurements.

### *Electrolyte Solutions*

All measurements were made in  $0.3 \text{ mol dm}^{-3} \text{ H}_3\text{BO}_3 + 0.075 \text{ mol dm}^{-3} \text{ Na}_2\text{B}_4\text{O}_7$  (pH = 8.4) prepared from *p.a.* chemicals and triply distilled water. The  $\text{K}_3\text{Fe}(\text{CN})_6$  and  $\text{K}_4\text{Fe}(\text{CN})_6$  were added directly into the solution in the form of strictly defined quantities of *p.a.* salts to obtain the required concentrations.

### *Working Electrodes*

A number of planar electrodes with the surface area of about  $0.2 \text{ cm}^2$  were made from a melt-spinning ribbons of  $\text{Fe}_{80}\text{B}_{20}$  (25  $\mu\text{m}$  thickness and 2.0 mm width), which were sealed into the glass holders. Only the shiny side of the ribbon was in contact with the electrolyte solution. The electrode surfaces had been polished by  $0.05 \mu\text{m}$   $\text{Al}_2\text{O}_3$ , and rinsed with methanol and triply distilled water, prior to being mounted into the electrolytic cell. Each electrode was passivated according to the strongly defined procedure.

### *Anodic Passive Film Formation Procedure*

Prior to passivation, each working electrode was cathodically polarized for 30 minutes at potential ( $E$ ) of about  $-0.80 \text{ V vs. SCE}$ , and at cathodic current densities of about  $0.1 \text{ mA/cm}^2$ . After that,  $E$  was scanned positively by  $0.3 \text{ mV/s}$  toward  $E = +0.20 \text{ V vs. SCE}$ , and then the potential scan was diminished to  $0.1 \text{ mV/s}$  until the film formation potential ( $E_f$ ),  $E = E_f = +0.60 \text{ V vs. SCE}$  was attained. The electrode was left on  $E_f$  until the anodic current density ( $i_a$ ) stopped changing appreciably, but for no less than 72 hours (three days). For a number of  $\text{Fe}_{80}\text{B}_{20}$  electrodes treated, the values were  $6 \pm 2 \times 10^{-5} \text{ mA/cm}^2$ . More details about the passivation procedure are given elsewhere.<sup>3,4</sup>

### *Steady-state Polarization of the Passivated Electrode*

»Quasi« steady-state polarization curves of working electrodes in the electrolyte solutions with and without redox couple were recorded between  $E = -0.20$  and  $E = +0.85 \text{ V vs. SCE}$ . The potential range between those limits agreed roughly with the potential range of full passivity for the passive  $\text{Fe}_{80}\text{B}_{20}$  electrode in the borate-buffered (pH = 8.4) blank solution.<sup>3</sup> The procedure was as follows: starting from  $E_f$ , the potential was scanned by  $10 \text{ mV/min}$  in an anodic direction up to  $E = +0.85 \text{ V vs. SCE}$ , where the electrode was left to equilibrate for about 30 minutes. Then, the »quasi« steady-state polarization curve was recorded by scanning potential in a cathodic direction by  $0.1 \text{ mV/s}$  until  $E = -0.20 \text{ V vs. SCE}$  was attained.

### *Impedance Measurements*

After the last point of the polarization curve was measured at  $E = -0.20 \text{ V vs. SCE}$ , the potential was returned upwards in  $0.025 \text{ V}$  anodic steps. On each potential step-point, impedance measurement was performed. Steady-state condition for impedance measurement was checked by replicate measurements at each potential

value. The highest anodic potential in the impedance measurements was  $E = +0.85$  V *vs.* SCE. After that point potential values were changed by 0.025 V steps in a cathodic direction, and the impedance measurements were repeated. The experimental apparatus and procedures were identical to those previously described.<sup>3,4</sup> In brief, Solartron-Schlumberger model 1250 FRA and model 1286 ECI, both equipped with an HP model 9816 computer, were used for the impedance measurements as a function of frequency ( $f = \omega/2\pi$ ) in the range between 20 kHz and 0.01 Hz. A signal of 10 mV peak-to-peak amplitude was used.

### Impedance Data Processing

All measured impedance data as a function of frequency were compared with the model impedance functions, determined from the corresponding electrical analogues. A theoretical data set for the chosen model function was generated by using a set of the predetermined parameter values. Each calculated data set was then fitted to the experimental data set. The modulus weighting procedure was not used. The best fits obtained by such a procedure are drawn in full lines in the relevant figures, while the impedance parameter values calculated from the best fits are listed in the corresponding tables. More details about impedance data processing are given elsewhere.<sup>3</sup>

## RESULTS

### »Quasi« Steady-state Polarization Curves

»Quasi« steady-state current-voltage curves of the passivated  $\text{Fe}_{80}\text{B}_{20}$  in the presence of 0.01 mol  $\text{dm}^{-3}$  ferri-ferrocyanide (in 1 : 1 molar ratio) redox couple in the borate-buffered (pH = 8.4) solution is displayed in Figure 1, together with the current-voltage curve of the passivated  $\text{Fe}_{80}\text{B}_{20}$  in the blank electrolyte solution (borate-buffered solution without redox couple).

As shown in Figure 1, the passive  $\text{Fe}_{80}\text{B}_{20}$  in the blank solution exhibits an almost potential independent steady-state faradaic current, which should be ascribed to the ionic (corrosion) current of the passive film.<sup>2-4</sup> However, in the presence of 0.01 mol  $\text{dm}^{-3}$  ferri-ferrocyanide redox couple, this current is diminished, and contributes significantly to the overall measured current at potentials between  $E > +0.05$  V and  $E < +0.50$  V *vs.* SCE. Outside these limits, the overall current density is markedly increased. The intersection point of the current density lines lies at  $E = +0.22$  V *vs.* SCE, which is in agreement with the literature value for the formal standard equilibrium potential ( $E_{\text{rev}}$ ) of the  $\text{Fe}(\text{CN})_6^{3-}/\text{Fe}(\text{CN})_6^{4-}$  redox couple.<sup>11,12</sup> Asymmetrical Tafel behaviour is obtained, being about -70 mV/decade in the range of cathodic potentials, and about 110 mV/decade in the anodic region. The terms cathodic or anodic potentials are *vs.*  $E_{\text{rev}} = +0.22$  V *vs.* SCE.

»Quasi« steady-state polarization curves for various concentrations of the ferri-ferrocyanide (in 1 : 1 molar ratio) redox couple are drawn in Figure 2, where the corresponding residual currents pertaining to the corrosion currents were subtracted prior to the drawings.

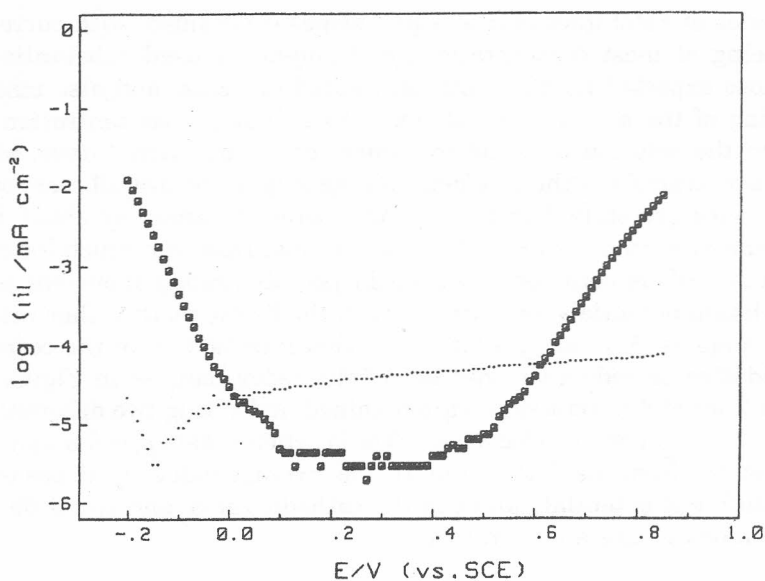


Figure 1. »Quasi« steady-state current-voltage dependencies of the passivated  $\text{Fe}_{80}\text{B}_{20}$ , measured in: (...) borate-buffered (pH = 8.4) blank solution; ( $\blacksquare$ ) borate-buffered (pH = 8.4) solution with  $0.01 \text{ mol dm}^{-3}$  ferri-ferrocyanide (in 1 : 1 molar ratio) redox couple.

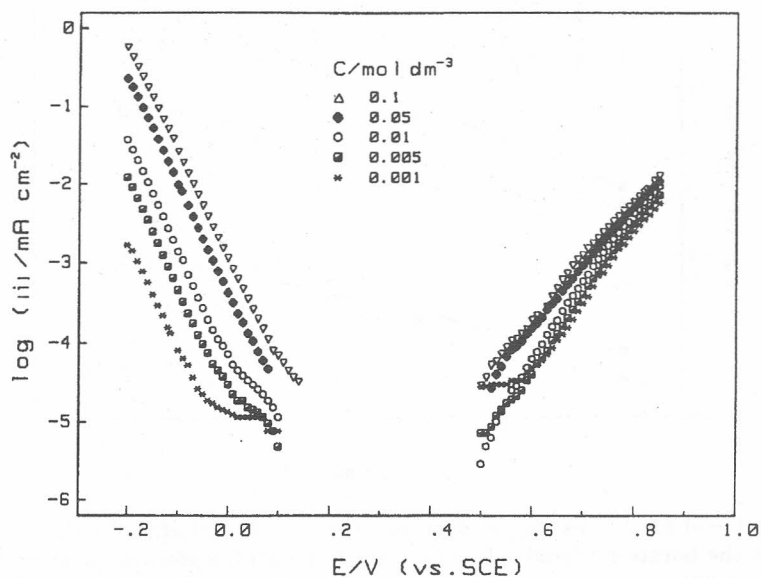


Figure 2. »Quasi« steady-state current-voltage dependencies of the passivated  $\text{Fe}_{80}\text{B}_{20}$ , measured in the borate-buffered (pH = 8.4) solution with denoted concentrations ( $c$ ) of the ferri-ferrocyanide (in 1 : 1 molar ratio) redox couple.

A series of Tafel lines of near equal slopes is obtained, with current densities being at most concentrations and potentials used substantially less than those expected for the diffusion limited currents, and also insensitive to stirring of the solution. All of this means that the concentration polarization in the solution does not influence the polarization curves, and that the electron transfer is the rate determining step in the overall reaction. Tafel dependencies are shifted in the cathodic potential range by about 100 mV per decade of concentration of the redox couple. However, much lower shifts of about 30 mV are obtained in the anodic potential range. If current densities at two chosen potentials (one within the cathodic range, the other within the anodic range *vs.*  $E_{\text{rev}}$ ) are presented *vs.* concentration ( $c$ ) of the corresponding (oxidative or reductive) member of the redox pair, as in Figure 3, two straight lines of different slopes are obtained, indicating two different values of the reaction order ( $p = \partial \log i / \partial \log c$ ). The reaction orders  $p_c = 0.6$  and  $p_a = 0.3$  are estimated from the data in Figure 3 as average values of slopes obtained at two different potential values in the cathodic range and two different potential values in the anodic range.

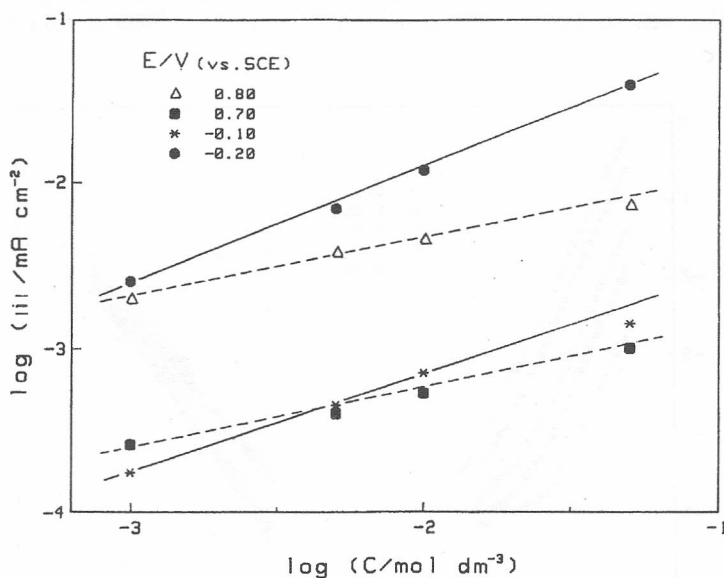


Figure 3. (—)  $\log |i|$  *vs.*  $\log$  of concentration ( $c$ ) of  $\text{Fe}(\text{CN})_6^{3-}$  for the passivated  $\text{Fe}_{80}\text{B}_{20}$  in the borate-buffered ( $\text{pH} = 8.4$ ) solution with the constant concentration of  $\text{Fe}(\text{CN})_6^{4-} = 0.001 \text{ mol dm}^{-3}$  at denoted potentials (*cathodic side vs.*  $E_{\text{rev}}$ ). (---)  $\log |i|$  *vs.*  $\log$  of concentration ( $c$ ) of  $\text{Fe}(\text{CN})_6^{4-}$  of the passivated  $\text{Fe}_{80}\text{B}_{20}$ , in the borate-buffered ( $\text{pH} = 8.4$ ) solution with a constant concentration of  $\text{Fe}(\text{CN})_6^{3-} = 0.001 \text{ mol dm}^{-3}$  at denoted potentials (*anodic side vs.*  $E_{\text{rev}}$ ).

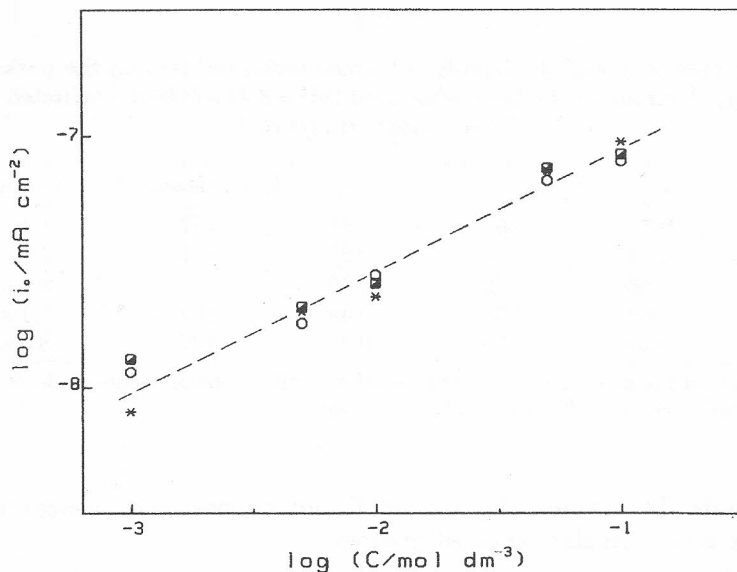


Figure 4.  $\log$  of the exchange current density ( $i_0$ ) values for a number of  $\text{Fe}_{80}\text{B}_{20}$  electrodes (denoted by different marks) vs.  $\log$  of concentration ( $c$ ) of the ferri-ferrocyanide (in 1 : 1 molar ratio) redox couple in the borate-buffered (pH = 8.4) solution.

The exchange current density values ( $i_0$ ) obtained from the intersection values of the corresponding cathodic and anodic lines in Figure 2 are drawn in Figure 4, as a function of the redox pair concentration (in 1 : 1 molar ratio). A number of different electrodes treated are denoted by different marks in Figure 4. Note also, that for all electrodes treated and all concentrations used, the intersection points fall at  $E = +0.22 \pm 0.02$  V vs. SCE.

In Table I, kinetic parameter values evaluated from the Tafel regions of the current-potential data in Figure 2 are listed, where cathodic ( $\alpha_c$ ) and anodic ( $\alpha_a$ ) transfer coefficients are calculated *via*:

$$\alpha_c = -2.3 RT/Fb_c \quad (1a)$$

$$\alpha_a = 2.3 RT/Fb_a \quad (1b)$$

In Eq. (1),  $b$  is a Tafel slope ( $b = dE/d\log i$ ) of the current-potential curve, while other symbols have their normal meaning.

The values of the »apparent« transfer coefficients and Tafel slopes from Table I do not appreciably change with the concentration of the ferri-ferrocyanide redox pair, particularly in the cathodic range of potentials. The values are, however, different in the cathodic range, compared to the anodic range

TABLE I

Kinetic parameters of the ferri-ferrocyanide redox reaction on the passivated Fe<sub>80</sub>B<sub>20</sub> electrode in the borate-buffered (pH = 8.4) solution, evaluated from Tafel regions in Figure 2

$c/\text{mol dm}^{-3}$	$\alpha_c$	$b_c/\text{mVdecade}^{-1}$	$\alpha_a$	$b_a/\text{mVdecade}^{-1}$	$i_o/\text{mA cm}^{-2}$
0.001	0.71	-83	0.55	107	$1.1 \times 10^{-8}$
0.005	0.84	-70	0.53	111	$2.0 \times 10^{-8}$
0.010	0.86	-69	0.50	118	$2.6 \times 10^{-8}$
0.050	0.80	-74	0.44	134	$7.1 \times 10^{-8}$
0.100	0.80	-74	0.43	137	$8.5 \times 10^{-8}$

\* The values of the parameters are average values of five measurements made at each concentration on two different Fe<sub>80</sub>B<sub>20</sub> electrodes.

of potentials. The values of  $i_o$  are small, but increase with concentration of the redox couple in the expected manner.<sup>10</sup>

#### Comparison with Data on Pure Passivated Iron

All the values listed in Table I are in rough agreement with those of Hackerman *et al.*<sup>11-13</sup> on their similarly prepared passive film on pure iron in the high overpotential conditions, and Schultze and Stimming<sup>15</sup> for their high thickness (> 25 nm) passive films at higher overpotentials. For pure iron passivated in a much shorter time (couple of hours), which implicates formation of a thinner passive film, the values of both transfer coefficients are found to be significantly lower.<sup>6,15,16</sup> The values of  $i_o$  from Table I are about several orders of magnitude lower than those obtained on the metal electrodes,<sup>6</sup> and about 20× lower than those obtained on the passivated pure Fe.<sup>11-13</sup>

#### Impedance

Frequency dependence of the passivated Fe<sub>80</sub>B<sub>20</sub> electrode impedance measured in the borate-buffered (pH = 8.4) solution with 0.01 mol dm<sup>-3</sup> ferri-ferrocyanide (in 1 : 1 molar ratio) redox couple, at some chosen potential values at the cathodic side of  $E_{\text{rev}}$ , are drawn in Figure 5 as Bode plots [ $\log |Z|$  vs.  $\log \omega$ , and phase angle vs.  $\log \omega$ ]. The impedance spectra measured in the blank solution in the same potential range are incorporated within Figure 5 for comparison purposes. Bode plots, but for some chosen potential values at the anodic side of  $E_{\text{rev}}$ , are drawn in Figure 6. For all the impedance spectra, the high-frequency resistance values pertaining almost to the electrolyte solution resistances, were subtracted prior to being drawn.<sup>17</sup>

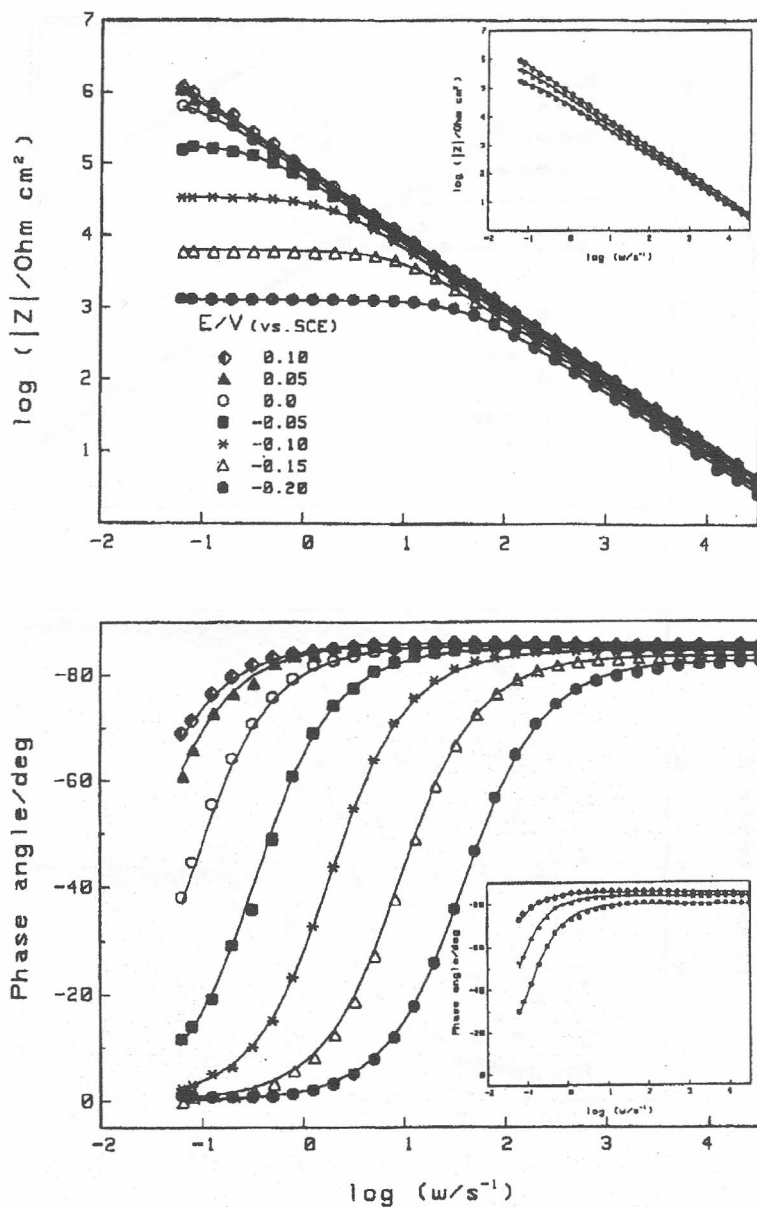


Figure 5. Bode plots of the passivated  $\text{Fe}_{80}\text{B}_{20}$  measured in the borate-buffered ( $\text{pH} = 8.4$ ) solution with  $0.01 \text{ mol dm}^{-3}$  ferri-ferrocyanide (in 1 : 1 molar ratio) redox couple, at denoted potentials (*cathodic side vs.  $E_{\text{rev}}$* ). Measured impedances are denoted by marks, the calculated impedances are denoted by full lines. All calculations are performed on the basis of Figure 9c with  $Z^*$  defined by the model in Figure 9a. Blank solution impedance data measured in the same potential region are drawn within the figure.

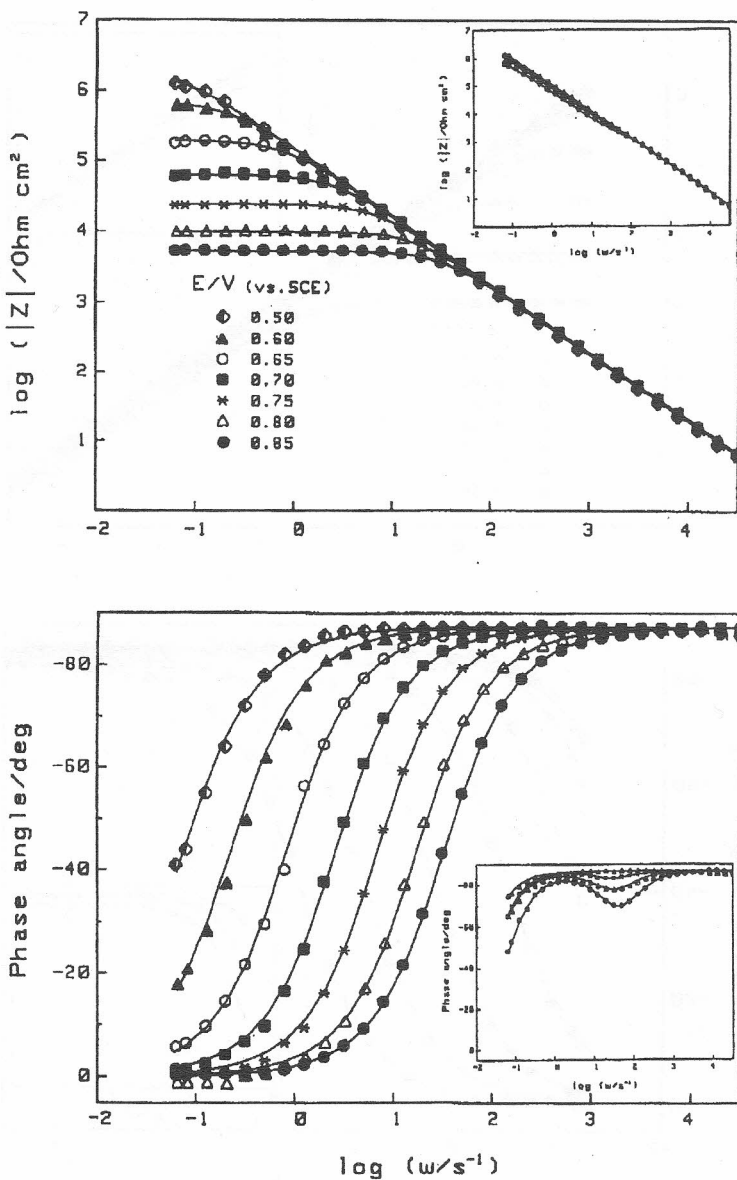


Figure 6. Bode plots of the passivated  $Fe_{80}B_{20}$  measured in the borate-buffered ( $pH = 8.4$ ) solution with  $0.01\ mol\ dm^{-3}$  ferri-ferrocyanide (in 1 : 1 molar ratio) redox couple at denoted potentials (anodic side vs.  $E_{rev}$ ). Measured impedances are denoted by marks, the calculated impedances are denoted by full lines. For  $E < +0.80\ V$  vs. SCE, the calculations are performed on the basis of Figure 9a, while for  $E \geq +0.80\ V$  vs. SCE,  $Z^*$  was defined according to the model in Figure 9b. Blank solution impedance data measured in the same potential region are drawn within the figure.

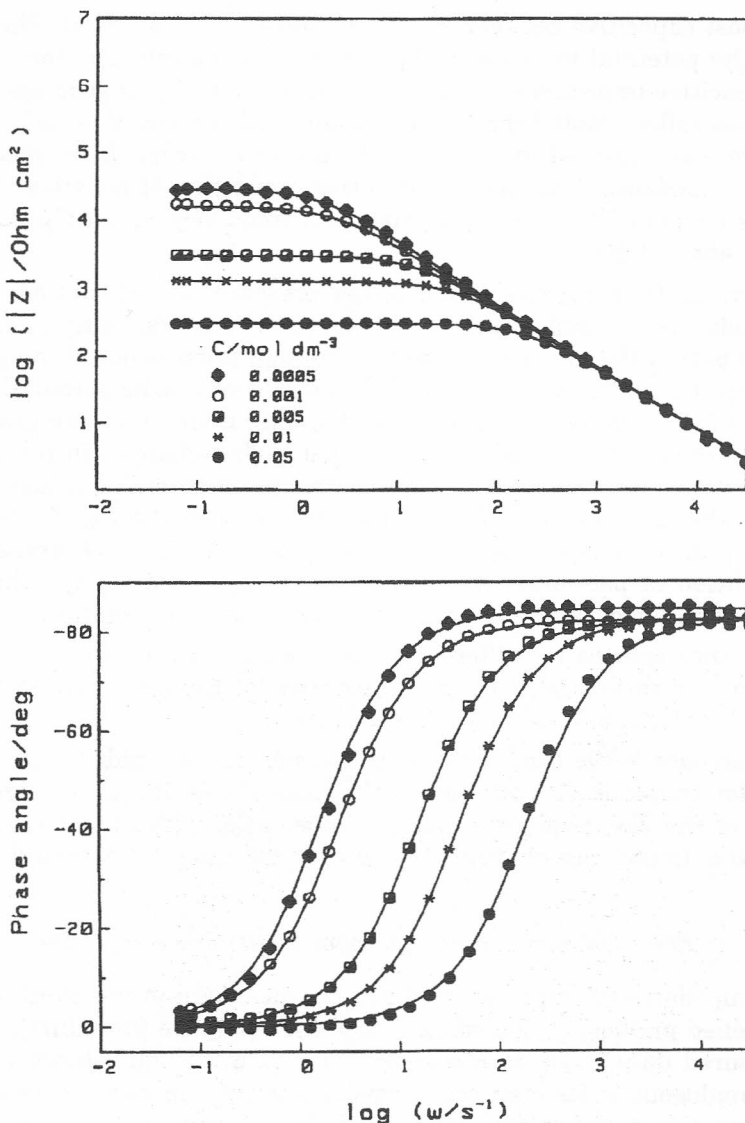


Figure 7. Bode plots of the passivated  $\text{Fe}_{80}\text{B}_{20}$  measured in the borate-buffered ( $\text{pH} = 8.4$ ) solution with denoted concentrations ( $c$ ) of the ferri-ferrocyanide (in 1 : 1 molar ratio) redox couple at  $E = -0.20$  V vs. SCE (cathodic side vs.  $E_{\text{rev}}$ ). Measured impedances are denoted by marks, the calculated impedances are denoted by full lines. All calculations are performed on the basis of Figure 9c with  $Z^*$  defined by the model in Figure 9a.

The potential dependence of the electrode impedance measured in the blank solution was discussed previously.<sup>3,4</sup> In brief, the impedance was found

to be almost capacitive between  $E = -0.20$  and  $+0.55$  V *vs.* SCE. The single effect of the potential increase in that range of potentials was the increase in the capacitive impedance as potential increases, being in good agreement with the »so called« Mott-Schottky behaviour. At  $E \geq +0.60$  V *vs.* SCE, a new impedance was observed in parallel with the former capacitive impedance. This new impedance consisted of the series connection of resistive ( $R_s$ ) and capacitive elements ( $C_s$ ), with the relaxation frequency ( $f_r = R_s C_s$ ) being observed at about 4 Hz.

As obvious from Figures 5 and 6, the presence of  $0.01 \text{ mol dm}^{-3}$  ferri-ferrocyanide (in 1 : 1 molar ratio) redox couple acts significantly on the low-frequency part of the impedance spectra, through prominence of the pure resistive impedance. By increase in either cathodic or anodic potential values referred to  $E_{\text{rev}}$ , this resistive impedance becomes more and more prominent in the overall impedance spectra. Somewhat higher changes in the low-frequency resistive impedance for the same change in potential values are obtained on the cathodic side of potentials. Inflexion in the  $\log |Z|$  *vs.*  $\log \omega$  plot, or dip in the phase angle *vs.*  $\log \omega$  plot at  $f \approx 4$  Hz, as observed in the blank solution at potentials  $E \geq +0.60$  V *vs.* SCE, is not visible when  $0.01 \text{ mol dm}^{-3}$  ferri-ferrocyanide is added into the electrolyte solution.

Impedance spectra for different concentrations of the ferri-ferrocyanide (in 1 : 1 molar ratio) redox couple are drawn in Figures 7 and 8 for  $E = -0.20$  V and  $+0.85$  V *vs.* SCE, respectively.

The increase in the concentration of the ferri-ferrocyanide (in 1 : 1 molar ratio) redox couple is for both potential values visible through a significant decrease of the low-frequency resistive impedance, with higher changes in the resistive impedance obtained in the cathodic range of potentials.

#### *The Electrical Equivalent Analogue of the Impedance Data*

The impedance of the passivated  $\text{Fe}_{80}\text{B}_{20}$  measured in the blank solution was modelled previously, according to a phase reference procedure based on the measured data.<sup>3,4</sup> Up to  $E = +0.55$  V *vs.* SCE, the impedance was considered analogous in its electrical properties to the constant phase element ( $\text{CPE}_i$ ) and the pure resistor ( $R_i$ ) situated in parallel connection. Use of CPEs instead of pure capacitors is a normal procedure when dealing with solid electrodes, which always exhibit a frequency dependence of capacitances.<sup>9,18</sup> Here, the CPE element is characterized by two parameters,  $K$  and  $\beta$  ( $0 < \beta \leq 1$ ), and its impedance ( $Z_{\text{cpe}}$ ) is defined according to:

$$Z_{\text{cpe}} = K^{-1}(i \omega)^{-\beta} \quad (2)$$

The electric analogue of the passivated  $\text{Fe}_{80}\text{B}_{20}$  electrode in the potential region between  $E = -0.20$  and  $E = +0.55$  V *vs.* SCE is drawn in Figure 9a,

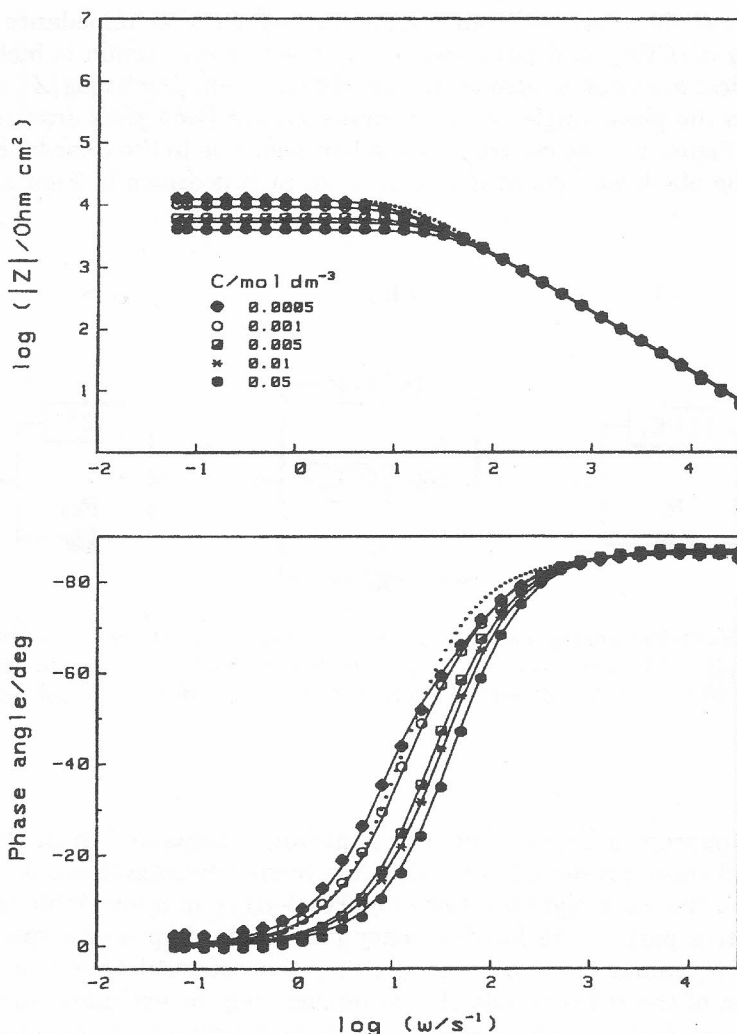


Figure 8. Bode plots of the passivated  $\text{Fe}_{80}\text{B}_{20}$  measured in the borate-buffered ( $\text{pH} = 8.4$ ) solution with denoted concentrations ( $c$ ) of the ferri-ferrocyanide (in 1 : 1 molar ratio) redox couple at  $E = +0.85$  V vs. SCE (anodic side vs.  $E_{\text{rev}}$ ). Measured impedances are denoted by marks, the calculated impedances are denoted by full lines. All calculations are performed on the basis of Figure 9c with  $Z^*$  defined by the model in Figure 9b. The calculated impedances performed on the basis of Figure 9c with  $Z^*$  defined by the model in Figure 9a, are for  $c = 0.0005$  mol  $\text{dm}^{-3}$  denoted in dots.

where  $(\text{CPE}_i)$  is considered as being an analogue to the interfacial capacitance, and  $R_i$  is considered analogous to the corrosion resistance of the passive film.

At  $E \geq +0.60$  V *vs.* SCE, an additional and parallel impedance branch consisting of (CPE<sub>s</sub>) and pure resistor R<sub>s</sub> in series connection is included in the electrical analogue to account for the obtained inflexion in  $\log|Z|$  *vs.*  $\log \omega$  and dip in the phase angle *vs.*  $\log \omega$  curves (*cf.* low Bode plots drawings comprised in Figure 6). The electrical equivalent analogue to the impedance measured in the blank solution at  $E \geq +0.60$  V *vs.* SCE is drawn in Figure 9b.

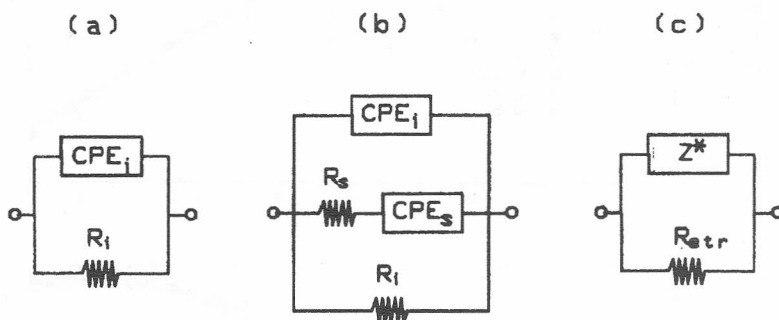


Figure 9. Electrical analogues of the passivated Fe<sub>80</sub>B<sub>20</sub> electrode: (a) in the borate-buffered (pH = 8.4) blank solution at  $E < +0.60$  V *vs.* SCE; (b) the same as (a) but for  $E \geq +0.60$  V *vs.* SCE; (c) with the ferri-ferrocyanide redox couple added.

The apparent difference between impedances measured in the blank solution and those presented here when the ferri-ferrocyanide redox couple is added into the electrolyte solution (Figures 5–8) is an appreciable change of the resistive part at the low-frequency part of the impedance spectra. Decrease of R<sub>i</sub> values with increase of either the potential values or the concentration of the redox couple should immediately be excluded, since corrosion current density values are found to be almost potential independent and significantly lowered as the concentration of the redox couple increases. Therefore, in order to explain the impedance spectra obtained, a new resistive element pertaining to the redox reaction of the redox couple has to be added in parallel to an already existing impedance. In Figure 9c, the equivalent electrical analogue for the passivated Fe<sub>80</sub>B<sub>20</sub> in solutions with the ferri-ferrocyanide redox couple added in the electrolyte solution is drawn, where by Z\* either electrical analogue in Figure 9a or that in Figure 9b is denoted, while by R<sub>etr</sub> the new resistive impedance due to the electron transfer reaction is accounted for. Thus, when the ferri-ferrocyanide redox couple is present in the electrolyte solution, the number of impedance parameters of the passivated Fe<sub>80</sub>B<sub>20</sub> electrode is increased only by one, if compared to those existing in the blank solution.

### The Impedance Parameter Values

The impedance parameter values obtained after the curve fitting procedure of the measured data drawn in Figures 5 and 6 and the impedance function of the electrical analogue in Figure 9c with  $Z^*$ , defined either by the model in Figure 9a or that in Figure 9b, are for all the potentials examined listed in Table II. The same, but for the data presented in Figures 7 and 8, are listed in Table III. The values of the measured current densities are also given in Tables II and III.

In the whole range of cathodic potentials ( $E < E_{\text{rev}}$ ) and at most anodic potentials ( $E > E_{\text{rev}}$ ), good fits are obtained if the impedances are calculated according to the model in Figure 9c, with  $Z^*$  defined by the model in Figure 9a (*cf.* full lines in Figures 5, 7 and those in Figure 6 for  $E < +0.80$  V *vs.* SCE). Here, the overall electrode impedance is generally described by four impedance parameter values (*cf.* the corresponding data listed in Tables II and III). Two of them ( $K_i, \beta_i$ ) are characteristic of the interfacial capacitance, and the other two are resistive and pertain to the ionic resistance ( $R_i$ ) and the electron transfer resistance ( $R_{\text{etr}}$ ). The number of the characteristic impedance parameters which could be obtained by the curve fitting procedure is in fact diminished to three ( $K_i, \beta_i, R$ ) since  $R_i$  and  $R_{\text{etr}}$  are in parallel connection, and thus only the value of their parallel sum  $R = R_i R_{\text{etr}} / (R_i + R_{\text{etr}})$  is available to estimations. However, the values of  $R_{\text{etr}}$  listed in Tables II and III are obtained by holding  $R_i$  values (estimated as  $R = R_i$  at potentials close to  $E_{\text{rev}}$  where  $R_{\text{etr}} \gg R_i$ ) constant during the calculations.

TABLE II

Current densities ( $i$ ) and impedance parameter values of the passivated  $\text{Fe}_{80}\text{B}_{20}$  electrode in the borate-buffered (pH = 8.4) solution and  $0.01 \text{ mol dm}^{-3}$  ferri-ferrocyanide (in 1 : 1 molar ratio) redox couple, at various potentials. Impedance parameter values were obtained by the curve fitting procedure of data in Figures 5 and 6

$E/V$ <i>vs.</i> SCE	$i$ $\text{mA cm}^{-2}$	$R_{\text{etr}}$ $\Omega \text{ cm}^2$	$K_i$ $\Omega^{-1} \text{ cm}^2 \text{ s}^{-\alpha_i}$	$\beta_i$	$R_i$ $\Omega \text{ cm}^2$	$K_s$ $\Omega^{-1} \text{ cm}^2 \text{ s}^{-\alpha_s}$	$\beta_s$	$R_s$ $\Omega \text{ cm}^2$
-0.20	$-2.5 \times 10^{-2}$	$1.3 \times 10^3$	$2.60 \times 10^{-5}$	0.92	$\sim 1 \times 10^7$	—	—	—
-0.15	$-7.2 \times 10^{-3}$	$6.3 \times 10^3$	$2.05 \times 10^{-5}$	0.93	$\sim 1 \times 10^7$	—	—	—
-0.10	$-1.3 \times 10^{-3}$	$3.4 \times 10^4$	$1.68 \times 10^{-5}$	0.94	$\sim 1 \times 10^7$	—	—	—
-0.05	$-2.6 \times 10^{-4}$	$1.9 \times 10^5$	$1.48 \times 10^{-5}$	0.95	$\sim 1 \times 10^7$	—	—	—
0	$-7.0 \times 10^{-5}$	$8.8 \times 10^5$	$1.31 \times 10^{-5}$	0.95	$\sim 1 \times 10^7$	—	—	—
+0.05	$-2.2 \times 10^{-5}$	$3.0 \times 10^6$	$1.17 \times 10^{-5}$	0.96	$\sim 1 \times 10^7$	—	—	—
+0.10	$-7.1 \times 10^{-6}$	$4.8 \times 10^6$	$1.10 \times 10^{-5}$	0.96	$\sim 1 \times 10^7$	—	—	—
+0.20	$-3.0 \times 10^{-6}$	—	$9.1 \times 10^{-6}$	0.97	$\sim 1 \times 10^7$	—	—	—
+0.30	$+1.1 \times 10^{-6}$	—	$8.0 \times 10^{-6}$	0.97	$\sim 1 \times 10^7$	—	—	—
+0.40	$+1.1 \times 10^{-6}$	—	$7.5 \times 10^{-6}$	0.97	$\sim 1 \times 10^7$	—	—	—
+0.50	$+6.1 \times 10^{-6}$	$5.0 \times 10^6$	$6.8 \times 10^{-6}$	0.97	$\sim 1 \times 10^7$	—	—	—
+0.60	$+8.3 \times 10^{-5}$	$6.1 \times 10^5$	$6.4 \times 10^{-6}$	0.97	$\sim 1 \times 10^7$	—	—	—
+0.65	$+2.3 \times 10^{-4}$	$1.9 \times 10^5$	$6.4 \times 10^{-6}$	0.97	$\sim 1 \times 10^7$	—	—	—
+0.70	$+5.7 \times 10^{-4}$	$6.4 \times 10^4$	$6.4 \times 10^{-6}$	0.97	$\sim 1 \times 10^7$	—	—	—
+0.75	$+1.6 \times 10^{-3}$	$2.5 \times 10^4$	$6.4 \times 10^{-6}$	0.97	$\sim 1 \times 10^7$	—	—	—
+0.80	$+4.1 \times 10^{-3}$	$1.0 \times 10^4$	$6.4 \times 10^{-6}$	0.97	$\sim 1 \times 10^7$	$\sim 2 \times 10^{-7}$	$\sim 0.95$	$\sim 2 \times 10^5$
+0.85	$+1.2 \times 10^{-2}$	$5.4 \times 10^3$	$6.6 \times 10^{-6}$	0.97	$\sim 1 \times 10^7$	$5 \times 10^{-7}$	0.95	$9 \times 10^4$

TABLE III

Current densities ( $i$ ) and impedance parameter values of the passivated  $\text{Fe}_{80}\text{B}_{20}$  electrode in the borate-buffered (pH = 8.4) solution and various concentrations ( $c$ ) of the ferri-ferrocyanide (in 1 : 1 molar ratio) redox couple, at  $E = -0.20$  V and  $E = +0.85$  V vs. SCE. Impedance parameter values were obtained by the curve fitting procedure of data in Figures 7 and 8

$c$ mol dm <sup>-3</sup>	$i$ mA cm <sup>-2</sup>	$R_{\text{etr}}$ $\Omega$ cm <sup>2</sup>	$K_i$ $\Omega^{-1}$ cm <sup>2</sup> s <sup>-<math>\alpha_i</math></sup>	$\beta_i$	$R_i$ $\Omega$ cm <sup>2</sup>	$K_s$ $\Omega^{-1}$ cm <sup>2</sup> s <sup>-<math>\alpha_s</math></sup>	$\beta_s$	$R_s$ $\Omega$ cm <sup>2</sup>
$E = -0.20$ V vs. SCE								
0.00	$-7.5 \times 10^{-5}$	—	$3.70 \times 10^{-5}$	0.89	$2 \times 10^5$	—	—	—
0.0005	$-1.0 \times 10^{-3}$	$2.9 \times 10^4$	$2.20 \times 10^{-5}$	0.94	$\sim 5 \times 10^6$	—	—	—
0.001	$-2.2 \times 10^{-3}$	$1.6 \times 10^4$	$2.75 \times 10^{-5}$	0.92	$\sim 6 \times 10^6$	—	—	—
0.005	$-1.1 \times 10^{-2}$	$3.1 \times 10^3$	$2.65 \times 10^{-5}$	0.92	$\sim 1 \times 10^7$	—	—	—
0.01	$-2.5 \times 10^{-2}$	$1.3 \times 10^3$	$2.60 \times 10^{-5}$	0.92	$\sim 1 \times 10^7$	—	—	—
0.05	$-1.1 \times 10^{-1}$	$3.1 \times 10^2$	$2.60 \times 10^{-5}$	0.92	$\sim 2 \times 10^7$	—	—	—
$E = +0.85$ V vs. SCE								
0.00	$8.6 \times 10^{-5}$	—	$8.3 \times 10^{-6}$	0.97	$\sim 1 \times 10^6$	$8.2 \times 10^{-6}$	0.94	$4.8 \times 10^3$
0.0005	$5.1 \times 10^{-3}$	$1.3 \times 10^4$	$6.8 \times 10^{-6}$	0.96	$\sim 5 \times 10^6$	$2.2 \times 10^{-6}$	0.95	$1.8 \times 10^4$
0.001	$6.2 \times 10^{-3}$	$9.6 \times 10^3$	$7.0 \times 10^{-6}$	0.96	$\sim 6 \times 10^6$	$1.4 \times 10^{-6}$	0.95	$2.8 \times 10^4$
0.005	$9.9 \times 10^{-3}$	$6.2 \times 10^3$	$6.7 \times 10^{-6}$	0.97	$\sim 1 \times 10^7$	$0.6 \times 10^{-6}$	0.95	$7.0 \times 10^4$
0.01	$1.2 \times 10^{-2}$	$5.4 \times 10^3$	$6.6 \times 10^{-6}$	0.97	$\sim 1 \times 10^7$	$0.5 \times 10^{-6}$	0.95	$9.0 \times 10^4$
0.05	$1.6 \times 10^{-2}$	$4.0 \times 10^3$	$6.8 \times 10^{-6}$	0.97	$\sim 2 \times 10^7$	$\sim 0.3 \times 10^{-6}$	$\sim 0.95$	$\sim 2 \times 10^5$

At higher anodic potentials, the quality of fits is significantly improved if  $Z^*$  defined by the model in Figure 9b is used instead of the one in Figure 9a. Differences are particularly evident at lower concentrations of the redox couple (*cf.* Figure 8). When the model in Figure 9b becomes operative, three additional parameters ( $K_s$ ,  $\beta_s$  and  $R_s$ ) pertaining to the appearance of a new parallel  $C_sR_s$  impedance increase the number of the characteristic electrode impedance parameters to seven. As obvious from the data in Tables II and III, the presence and increase of the potential and concentration of the ferri-ferrocyanide redox couple have a significant influence on the values of  $R_s$  and  $K_s$ , but not on the relaxation frequency ( $f_r \approx 4$  Hz) of the  $C_sR_s$  impedance. Increase of the  $C_sR_s$  impedance with an increase in the concentration of the redox couple is just the reason why the  $C_sR_s$  impedance is either more weakly, or not at all, seen in Bode plots, if compared with impedances measured in the blank solution.

## DISCUSSION

### *The Blank Solution Behaviour*

According to the results obtained previously,<sup>3</sup> the passivated  $\text{Fe}_{80}\text{B}_{20}$  in near neutral borate-buffered solutions exhibits n-type semiconductive properties with a space charge in the electron depletion form in almost the whole

passive potential region (between  $-0.20$  and  $+0.55$  V *vs.* SCE). In that range of potentials, the change in the external voltage is manifested through a change in the potential drop across the space-charge region ( $\Delta\phi_{sc}$ ), while the potential drop across the ionic Helmholtz layer ( $\Delta\phi_H$ ) remains in equilibrium, which is defined by the electrolyte solution pH dependent protolytic dissociation of the surface adsorbed hydroxyl groups. The »quasi« steady-state current-potential dependence exhibits an almost potential independent anodic current density (Figure 1) due to an ionic (corrosion) current. The analysis of impedance data has revealed the values of the ionic (corrosion) transfer resistance ( $R_i$ ) and interfacial capacitance ( $K_i \approx C_i$ ) as a nonseparable sum of the space-charge capacitance ( $C_{sc}$ ) and the Helmholtz double-layer ionic capacitance ( $C_H$ ). From the Mott-Schottky potential dependence of  $C_i$  values, the flat-band potential ( $E_{fb}$ ) of the passive  $Fe_{80}B_{20}$  is estimated to be  $-0.38$  V *vs.* SCE in the pH = 8.4 solution.

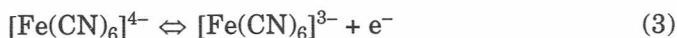
At higher potentials (between  $+0.60$  and  $+0.85$  V *vs.* SCE), owing to the surface deprotonation reaction, there is an increased density of the adsorbed basic hydroxyl groups acting as surface states. The density of surface states influences  $C_i$  significantly and causes breaks of the Mott-Schottky dependence. The oxidation reaction of surface states starts just below the OER region, being observable through appearance of a new  $C_s R_s$  impedance. The formed oxidized species act as intermediates in the subsequent OER reaction, which proceeds at  $E > +0.85$  V *vs.* SCE, and is accompanied by the Tafel behaviour of the current-potential curve as well as by the low-frequency resistive behaviour of the overall impedance spectra.

### *Mechanism of the Interfacial Electron Transfer Process*

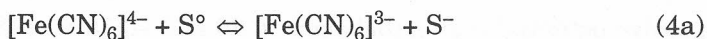
If the ferri-ferrocyanide redox couple is present in the electrolyte solution, the electron transfer occurs at either cathodic or anodic potentials relative to  $E_{rev}$ , as shown by Tafel dependencies in Figures 1 and 2. At potentials close to  $E_{rev}$ , the current densities are very small and equal within an order of magnitude to the values of the ionic (corrosion) current densities.

Generally, there are two ways of the electron transfer between the passive film and ferri-ferrocyanide redox couple in the solution.<sup>12,19</sup> These are:

(i) Direct electron transfer which proceeds in a single step according to the following reaction:



(ii) Indirect electron transfer, or mediation of electron transfer *via* surface states (S), which proceeds according to the following two-step mechanism:



In both cases, electrons have to pass across the passive film and the current density, being an ionic current density ( $i_i$ ) in the blank solution, is increased due to the increase of the electronic part ( $i_{\text{etr}}$ ):

$$i = i_i + i_{\text{etr}} \quad (5)$$

In Eq. (5),  $i_{\text{etr}}$  has to be considered as being the sum of its cathodic ( $i_c$ ) and anodic ( $i_a$ ) parts, with  $i_c$  pertaining to the electroreduction reaction of the ferricyanide ions, and  $i_a$  pertaining to the electrooxidation reaction of the ferrocyanide ions. As usual in the electrode kinetics, both reactions proceed at equal rates at  $E = E_{\text{rev}}$ , with the characteristic exchange current density ( $i_o$ ), or with the equivalent resistance  $R_o$ , being defined as:<sup>20</sup>

$$R_o \text{ (at } E_{\text{rev}} \text{ and } f \rightarrow 0) = RT / Fi_o \quad (6)$$

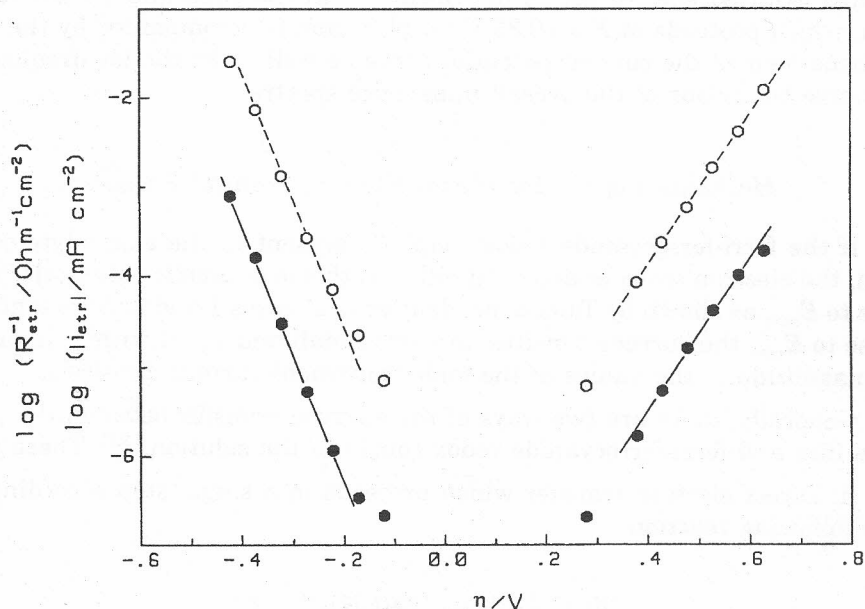


Figure 10. (—)  $\log(R_{\text{etr}}^{-1})$  vs.  $\eta$  of the passivated  $\text{Fe}_{80}\text{B}_{20}$  electrode in the borate-buffered (pH = 8.4) solution and  $0.01 \text{ mol dm}^{-3}$  ferri-ferrocyanide redox couple. (---)  $\log |i_{\text{etr}}|$  vs.  $\eta$  of the passivated  $\text{Fe}_{80}\text{B}_{20}$  electrode in the borate-buffered (pH = 8.4) solution and  $0.01 \text{ mol dm}^{-3}$  ferri-ferrocyanide redox couple.

In Tafel regions, however, when the back reaction can be neglected,

$$i_{\text{etr}} = i_0 \exp(\eta/b) \quad \text{or} \quad \log i_{\text{etr}} = \log i_0 + \eta/b \quad (7)$$

and

$$R_{\text{etr}}^{-1} = (i_0/b) \exp(\eta/b) \quad \text{or} \quad \log(R_{\text{etr}}^{-1}) = \log(i_0/b) + \eta/b \quad (8)$$

$\eta$  from Eqs. (7–8) denotes an overpotential term, being zero at  $E_{\text{rev}}$  of the redox couple, *i.e.*  $\eta = E - E_{\text{rev}}$ .  $R_{\text{etr}}$  from Eq. (8) is the electron transfer reaction resistance, which should be obtained from the low-frequency impedance measurements. Determinations of  $R_{\text{etr}}$  by impedance measurements are thus fully equivalent to the conventional steady-state current-potential measurements, which is corroborated by Figure 10, where equal Tafel dependencies are obtained if presented either according to Eq. (7) as  $\log |i_{\text{etr}}|$  *vs.*  $\eta$ , or according to Eq. (8) as  $\log R_{\text{etr}}^{-1}$  *vs.*  $\eta$ .

#### *Interfacial Electron Transfer in the Cathodic Region*

Values of the apparent cathodic kinetic parameters ( $\alpha_c$  and  $b_c$ ) listed in Table I, their independence of the concentration of the redox couple, together with the concentration and potential dependence of the corresponding  $R_{\text{etr}}$  values from Tables II and III, resemble roughly the isoenergetic electron transfer mechanism, characteristic of the semiconductor of n-type.<sup>5–8</sup> In an ideal case of such behaviour,  $\alpha_c = 1$  ( $b_c = -60$  mV/decade) is expected for the simple one-electron transfer reduction reaction. Also, the current has to be linearly proportional to the concentration of oxidant ( $p_c = \partial \log i_c / \partial \log c = 1$ ) and cannot give a saturation behaviour.<sup>5,6–8</sup> From impedance measurements a  $-60$  mV/decade Tafel slope from the potential dependence of  $R_{\text{etr}}$  values, and potential independent  $C_i$  values due to the passive film and ionic Helmholtz double-layer capacitances in series connection are expected. For this mechanism, the reduction reaction of the ferricyanide ions should be written as reaction (3) in its back direction, with electrons ( $e^-$ ) being surface electrons from the conduction band.

Although the present results are not sufficient to reveal fully this mechanism ( $\alpha_c \approx 0.80$ ,  $b_c \approx -75$  mV/decade,  $p_c \approx 0.6$ , potential dependent  $K_i$ ), a back direction of reaction (3) can be still warranted as being the dominant reaction in electroreduction of the ferricyanide ions on the passivated  $\text{Fe}_{80}\text{B}_{20}$ . However, discrepancies from the ideal behaviour could be explained in the following manner:

- At cathodic potentials (between  $-0.20$  and about  $0.00$  V *vs.* SCE), where the Tafel behaviour is observed (*cf.* Figures 1 and 2), the passive film on  $\text{Fe}_{80}\text{B}_{20}$  is anodically biased relative to  $E_{\text{fb}}$ , and there is an electron depletion surface layer acting as a potential barrier, which is evident

from the characteristic Mott-Schottky potential dependence of  $K_i$  ( $C_i$ ) values. Contribution of the tunnelling of electrons, although relatively low at low  $\eta$ , could possibly be the reason for  $\alpha_c < 1$  ( $|b_c| > 60$  mV/decade).<sup>6</sup>

- There is also a possibility that the electron transfer reaction is, at least partly, a two-step mechanism,<sup>12,21,22</sup> *i.e.* it partly proceeds according to the back direction of Eq. (4), which also results in the overall  $\alpha_c$  and  $p_c < 1$
- In a range of potentials between  $-0.20$  and about  $0.00$  V *vs.* SCE, the overall potential drop of the passivated  $\text{Fe}_{80}\text{B}_{20}$ /solution interface ( $\Delta\phi_{\text{F/S}}$ ) is partitioned over the space-charge ( $\Delta\phi_{\text{sc}}$ ) and ionic part of the double-layer ( $\Delta\phi_{\text{H}}$ ).<sup>3,4</sup> Contribution of the electron tunnelling through the ionic part of double-layer could also decrease  $\alpha_c$  and  $p_c$  values.<sup>12</sup> However, this contribution seems to be less probable in our situation, due to the constant and potential independent  $\Delta\phi_{\text{H}}$  in this range of potentials.<sup>3,4</sup>

### *Interfacial Electron Transfer in the Anodic Region*

Kinetic parameters from Table I are estimated for the potential range between about  $+0.55$  and  $+0.85$  V *vs.* SCE (*cf.* Figures 1 and 2). They offer  $\alpha_a \cong 0.5$  ( $b_a \cong 120$  mV/decade), being slightly dependent on the concentration of the redox couple.  $i_a$  and  $R_{\text{etr}}^{-1}$  from the corresponding parts of Tables II and III are proportional to the concentration of the redox couple, and the anodic reaction order,  $p_a$ , is estimated to be  $\approx 0.3$  (*cf.* Figure 3). The corresponding  $K_i$  values from Tables II and III are almost not dependent on either the potential or concentration of the redox-couple.

The isoenergetic electron transfer from the conduction band proceeding *via* reaction (3) should provide a purely blocking behaviour on the anodic side of  $E_{\text{rev}}$ , due to strong electron depletion conditions, the behaviour already observed on valve metals.<sup>5-8</sup> In that case,  $\alpha_a$  should be equal to 0 ( $b_a = \infty$ ). Consequently, no dependence of kinetic data on the concentration of redox species could be observed. The transfer coefficient  $\alpha_a > 0$  may be explained in terms of this mechanism, if the essential part of space-charge depletion layer is transparent for conduction band electrons by way of the tunnelling effect, as it has been observed for a case of thin barriers insured by high concentration of electron donor species.<sup>6</sup> The alternative valence band mechanism with the reversed transfer coefficients:  $\alpha_c = 0$  and  $\alpha_a = 1$  should be rejected here, since this mechanism is not common for the n-type of semiconductors at not too high anodic potentials, due to the energetic position of their valence band.<sup>5,6</sup>

In an ideal case,  $\alpha_a = 0.5$  ( $b_a = 120$  mV/decade) and  $p_a = 1$  are expected for the simple one-electron oxidation reaction as is reaction (3) in its forward direction, proceeding on the metal-type electrodes,<sup>5-7</sup> and also on metals where hydrous oxide films of excellent electronic conductivities are formed.<sup>6,23,24</sup> For both kinds of electrodes, the total potential drop is utilized within  $\Delta\phi_{\text{H}}$ , the rates of redox reactions are high, and Tafel behaviour is usu-

ally influenced by the solution concentration polarization effects. Here, for the passivated  $\text{Fe}_{80}\text{B}_{20}$ , much lower current densities are measured, which together with very low  $i_0$  values indicate a significant influence of the passive film on the electron transfer. No appreciable current saturation effects are observed either, indicating the electron transfer step to be rate determining at all potentials and concentrations of the redox couple examined. This is corroborated by impedance measurements, where pure resistive low-frequency impedances with no appreciable Warburg impedance contribution (*cf.* Figures 6 and 8) are observed.

The values of the transfer coefficient  $\alpha_a$  and the reaction order  $p_a$  as observed may be explained, however, if the faradaic current transport proceeds *via* surface states,<sup>12,21,22</sup> *i.e.* if the oxidation reaction is described by the reaction (4) in its forward direction. By reaction (4a) ferrocyanide ions transfer their electrons to the electron unoccupied surface states ( $\text{S}^\circ$ ), while by reaction (4b) there is a transfer of electrons from occupied surface states ( $\text{S}^-$ ) to the interior of the passive film. As usual in the electrochemical kinetics, the overall reaction rate is determined by the rate of the slowest step.

In impedance measurements, a single step kinetically controlled electron transfer described by reaction (3) is expected to be seen as a pure resistive impedance, being dominant at lower frequencies. The same impedance spectra shape is expected for a two step electron transfer mechanism described by reaction (4), for the case of no significant contribution of the surface charging/discharging enabled by formation and ionization of  $\text{S}^-$  species. In such a case, the low frequency resistive impedance is a series sum of two resistance values belonging to reactions (4a) and (4b), where usually the highest resistance value determines the overall sum. If there is a significant contribution of additional charges, however, an inflection in  $\log |Z|$  and dip in the phase angle representations of Bode plots is expected, but only when the second step reaction is either fully inhibited or rate determining. Those effects were indeed observed<sup>3,4</sup> in impedance measurements of the passivated  $\text{Fe}_{80}\text{B}_{20}$  electrode in the blank (pH = 8.4) solution at higher anodic potentials, where a new additional  $R_s C_s$  impedance with  $f_r \approx 4\text{Hz}$  was ascribed to the oxidation of surface adsorbed hydroxyl ions according to:



A possibility that reaction (9a) is the first step of the ferrocyanide oxidation reaction being followed by the second-step reaction



could be rejected as being operative in describing the oxidation of ferrocyanide ions on the passivated  $\text{Fe}_{80}\text{B}_{20}$  electrode surface for the following three reasons:

(i) According to data in Figure 2, for the concentration range of the redox couple used, the Tafel behaviour due to the oxidation reaction of ferrocyanide ions ( $E > E_{\text{rev}}$ ) becomes observable between +0.40 and +0.50 V *vs.* SCE. These potential values are lower than  $E \geq +0.60$  V *vs.* SCE where the reaction of  $\text{OH}^\circ$  formation is usually observed through appearance of an additional  $R_s C_s$  impedance with  $f_r \approx 4\text{Hz}$ , in either blank (pH = 8.4) solution<sup>3,4</sup> or in the solution with the redox couple added (Tables II and III).

(ii) The reaction (9a) should not be considered as being catalyzed by the presence of the redox couple in the electrolyte solution. In contrast, impedance parameter values from the data in Tables II and III point to an increase of the impedance values, *i.e.* there is an inhibition of the reaction (9a) if the redox couple is present in the electrolyte solution.

(iii) The curve fitting procedure of the measured data and impedance function calculated for the model, which takes into account a series connection of  $R_s$  and  $R_{\text{etr}}$  values, yielded less agreement between the calculated and measured data than obtained here, where impedance calculations are based on the parallel connection of two resistances (*cf.* model in Figure 9c with  $Z^*$  defined by model in Figure 9b).

From all that have been said above, it seems that oxidation of ferrocyanide ions on the passivated  $\text{Fe}_{80}\text{B}_{20}$  electrode should generally be described by reaction (4), where surface states involved are not adsorbed basic hydroxyl groups. As already postulated in the literature for the passivated iron,<sup>19</sup> ferrocyanide ions act as more efficient donors of electrons to the positive electrode surface than adsorbed  $\text{OH}^-$ , whose oxidation as a competitive electrode reaction is strongly inhibited and observed at a much higher anodic potential in the presence of the redox couple than in the blank solution.

The unoccupied surface states ( $\text{S}^\circ$ ) involved in reaction (4) should probably be ionized donors (*e.g.* surface point defects) whose concentration increases with anodic potential. These surface states capture electrons by reaction (4a) and deliver electrons by reaction (4b). For such a case, the »apparent« transfer coefficients and anodic reaction order are under the strong influence of all potential dependent quantities, such as rate constants, surface state density, or the capture coefficient, and may attain a wide spectra of different values, including those observed here.<sup>12,21,22</sup>

## CONCLUSIONS

Potential dependence of the »quasi« steady-state current density and low-frequency resistance of the impedance, measured between  $-0.20$  and  $+0.85$  V *vs.* SCE on the passivated  $\text{Fe}_{80}\text{B}_{20}$  electrode in the borate-buffered (pH = 8.4) solution in the presence of the ferri-ferrocyanide redox couple, shows that redox reaction exhibits two linear Tafel regions, one in the

cathodic, the other in the anodic range relative to  $E_{\text{rev}}$ . There is no appreciable influence of the solution concentration polarization effects in the range of concentration of the redox couple used, indicating electron transfer to be the rate determining step of the overall reaction. The rates of both reactions and values of the exchange current densities are still lower than those usually obtained on the oxide covered electrodes. Impedance measurements and subsequent data analysis point to the kinetically controlled faradaic process situated in parallel with an already existing impedance of the blank solution, in either cathodic or anodic range of potentials. In both ranges of potential *vs.*  $E_{\text{rev}}$  of the redox couple, the redox reaction proceeds dominantly *via* isoenergetic electron transfer between the conduction band of the n-type semiconductor-like passive film and ions in the solution. At cathodic potentials *vs.*  $E_{\text{rev}}$  of the redox couple, contributions of either electron tunnelling across an electron depletion space-charge layer and/or surface state mediation are possible reasons for the observed discrepancies from ideal behaviour. At anodic potentials *vs.*  $E_{\text{rev}}$  of the redox couple, in the conditions of a high surface electron depletion, the contribution of surface states mediation is high. Oxidation of ferrocyanide ions proceeds mainly *via* surface states, probably ionized donor species (*e.g.* oxide lattice point defects). It seems that ferrocyanide ions are more efficient donors of electrons to the positive surface than are the surface adsorbed basic hydroxyl ions, which is observed through inhibition of the oxidation reaction of the hydroxyl ions if the redox couple is present in the electrolyte solution.

Comparison with kinetic data obtained on the passivated iron shows rough agreement between two passive films, but only if iron-passive films of sufficient thickness are compared. About 20× lower exchange current density values than obtained for the passivated  $\text{Fe}_{30}\text{B}_{20}$ , point to the significantly lower catalytic efficiency of the  $\text{Fe}_{30}\text{B}_{20}$  passive film surface.

*Acknowledgement.* – This work is supported by the Ministry of Science of the Republic of Croatia (Project No. 1-07-162).

## REFERENCES

1. D. Hodko, K. Kvastek, V. Horvat, and V. Pravdić, *Croat. Chem. Acta* **64** (1991) 111.
2. K. Kvastek, V. Horvat-Radošević, D. Hodko, and V. Pravdić, *Electrochim. Acta* **38** (1993) 205.
3. V. Horvat-Radošević, K. Kvastek, D. Hodko, and V. Pravdić, *Electrochim. Acta* **39** (1994) 119.
4. V. Horvat-Radošević and K. Kvastek, *Electrochim. Acta* **42** (1997) 1403.
5. S. R. Morrison, *Electrochemistry at Semiconductor and Oxidized Metal Electrodes*, Plenum Press, New York, 1980.

6. W. Schmickler and J. W. Schultze, in: J. O'M. Bockris, B. E. Conway, and R. E. White (Eds.), *Modern Aspects of Electrochemistry*, No. 17, Plenum Press, New York 1986, p. 357.
7. J. W. Schultze and L. Elfenthal, *J. Electroanal. Chem.* **204** (1986) 153.
8. H. Gerischer, *Electrochim. Acta* **35** (1990) 1677.
9. J. R. Macdonald (Ed.), *Impedance Spectroscopy*, J. Wiley, New York, 1987.
10. R. V. Motshev, *Electrochim. Acta* **16** (1971) 2039.
11. S. M. Wilhelm, K. S. Yun, L. W. Ballenger, and N. Hackerman, *J. Electrochem. Soc.* **126** (1979) 419.
12. F. M. Delnick and N. Hackerman, *J. Electrochem. Soc.* **126** (1979) 732.
13. S. M. Wilhelm and N. Hackerman, *J. Electrochem. Soc.* **128** (1981) 1668.
14. U. Stimming and J. W. Schultze, *Electrochim. Acta* **24** (1979) 859.
15. J. W. Schultze and U. Stimming, *Z. Phys. Chem. N. F.* **98** (1975) 285.
16. E. B. Castro and J. R. Vilche, *Electrochim. Acta* **38** (1993) 1567.
17. M. Sluyters-Rehbach and J. H. Sluyters in: E. Yeager, J. O'M. Bockris, B. E. Conway, and S. Sarangapani (Eds.), *Comprehensive Treatise of Electrochemistry*, Plenum Press, New York, 1984, Vol. 9, p. 177.
18. X. Wu, W. Zhang, and H. You, *J. Electroanal. Chem.* **398** (1995) 1.
19. L. M. Abrantes and L. M. Peter, *J. Electroanal. Chem.* **150** (1983) 593.
20. B. D. Cahan and C. T. Chen, *J. Electrochem. Soc.* **129** (1982) 700.
21. V. A. Tyagai and G. Ya. Kolbasov, *Surface Sci.* **28** (1971) 423.
22. W. P. Gomes and D. Vanmaekelbergh, *Electrochim. Acta* **41** (1996) 967.
23. R. F. Savinelli, R. L. Zeller, and J. A. Adams, *J. Electrochem. Soc.* **137** (1990) 489.
24. D. Marijan and M. Vuković, *Croat. Chem. Acta* **67** (1994) 297.

## SAŽETAK

### Kinetika reakcije $[\text{Fe}(\text{CN})_6]^{3-}/[\text{Fe}(\text{CN})_6]^{4-}$ redoks para na anodno pasiviziranom $\text{Fe}_{80}\text{B}_{20}$

*Višnja Horvat-Radošević, Krešimir Kvastek i Dejana Križekar*

Ispitivana je redoks-reakcija različitih koncentracija (u 1 : 1 množinskom omjeru) redoks-para  $[\text{Fe}(\text{CN})_6]^{3-}/[\text{Fe}(\text{CN})_6]^{4-}$  u neutralnoj otopini boratnog pufera (pH = 8.4), na  $\text{Fe}_{80}\text{B}_{20}$  elektrodi pasiviziranoj pod strogo određenim uvjetima. Izvršena su potencijostatska mjerenja impedancije i kvazi-stacionarna polarizacijska mjerenja. Rezultati mjerenja jasno pokazuju da je u oba smjera (katodnom i anodnom) s obzirom na  $E_{\text{rev}}$  redoks-para, prijenos elektrona ona reakcija koja određuje brzinu ukupnog procesa. Brzine reakcija kao i veličina struje izmjene su malene, ali su svojstvene oksidnim elektrodama. Analiza impedancije pokazuje da je reakcija prijenosa elektrona u paraleli s postojećom međufaznom (pasivni film/otopina) impedancijom u otopini bez redoks-para. Redoks-reakcija odvija se na pasiviziranom  $\text{Fe}_{80}\text{B}_{20}$  uglavnom putem prijenosa elektrona između vodljive vrpce i iona u otopini, što je karakteristično za klasični poluvodič n-tipa. Odstupanje od idealnog ponašanja u katodnom području, može se objasniti doprinosom tuneliranja elektrona kroz tanki sloj nastaloga prostornog naboja, i/ili djelomičnom reakcijom prijenosa elektrona putem površinskih stanja. U anodnom

području potencijala, kada je sloj prostornog naboja (koji djeluje kao visoka površinska barijera) deblji, doprinos prijenosa elektrona preko površinskih stanja, stvorenih potencijalno ovisnom ionizacijom donora unutar pasivnog filma je velik. U oba područja potencijala, brzina reakcije određena je svojstvima graničnog područja unutar pasivnog filma, a ne graničnog područja s otopinske strane međufaze, stvorene između pasivnog filma i otopine elektrolita. Usporedba s literaturnim podacima za (deblje) pasivne filmove formirane na čistom željezu, pokazuje sličnost u kinetičkim parametrima, ali i slabiju katalitičku efikasnost površine pasivnog filma na  $\text{Fe}_{80}\text{B}_{20}$ .